NEURAL REGENERATION RESEARCH
www.nrronline.org

Research Article

Ischemic accumulation of succinate induces Cdc42 succinylation and inhibits neural stem cell proliferation after cerebral ischemia/reperfusion

Lin-Yan Huang[1, #], Ju-Yun Ma[2, #], Jin-Xiu Song[2, #], Jing-Jing Xu[1], Rui Hong[1], Hai-Di Fan[2], Heng Cai[2], Wan Wang[1], Yan-Ling Wang[1], Zhao-Li Hu[3], Jian-Gang Shen[1, 4], Su-Hua Qi[1, 2, 3, *]

https://doi.org/10.4103/1673-5374.355821

Date of submission: October 18, 2021

Date of decision: February 8, 2022

Date of acceptance: August 10, 2022

Date of web publication: October 10, 2022

From the Contents

Introduction	1040
Methods	1041
Results	1042
Discussion	1043

Graphical Abstract

Effects of succinate accumulation on neural stem cell proliferation after cerebral ischemia/reperfusion injury

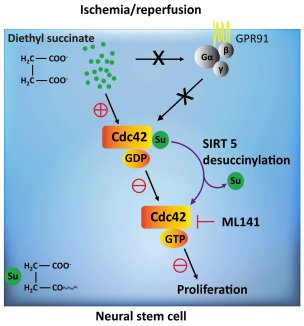

Abstract

Ischemic accumulation of succinate causes cerebral damage by excess production of reactive oxygen species. However, it is unknown whether ischemic accumulation of succinate affects neural stem cell proliferation. In this study, we established a rat model of cerebral ischemia/reperfusion injury by occlusion of the middle cerebral artery. We found that succinate levels increased in serum and brain tissue (cortex and hippocampus) after ischemia/reperfusion injury. Oxygen-glucose deprivation and reoxygenation stimulated primary neural stem cells to produce abundant succinate. Succinate can be converted into diethyl succinate in cells. Exogenous diethyl succinate inhibited the proliferation of mouse-derived C17.2 neural stem cells and increased the infarct volume in the rat model of cerebral ischemia/reperfusion injury. Exogenous diethyl succinate also increased the succinylation of the Rho family GTPase Cdc42 but repressed Cdc42 GTPase activity in C17.2 cells. Increasing Cdc42 succinylation by knockdown of the desuccinylase Sirt5 also inhibited Cdc42 GTPase activity in C17.2 cells. Our findings suggest that ischemic accumulation of succinate decreases Cdc42 GTPase activity by induction of Cdc42 succinylation, which inhibits the proliferation of neural stem cells and aggravates cerebral ischemia/reperfusion injury.

Key Words: Cdc42; cerebral ischemia/reperfusion injury; GPR91; neural stem cells; neurogenesis; proliferation; SIRT5; succinate; succinylation

Introduction

Cerebral ischemia/reperfusion (I/R) occurs when the cerebral blood supply is disrupted and then restored. Reperfusion initiates oxidative damage and cell death by generation of mitochondrial reactive oxygen species (Eltzschig and Eckle, 2011). Production of mitochondrial reactive oxygen species is driven by ischemic accumulation of succinate, an intermediate of the citric acid cycle (Chouchani et al., 2014; Kamarauskaite et al., 2020; Zhang et al., 2020; Zhu et al., 2021). Under aerobic conditions, intracellular succinate is rapidly metabolized into fumarate. Under anaerobic conditions, elevated levels of extracellular succinate bind to and activate the G protein-coupled succinate receptor GPR91 on stellate cells and macrophages in the liver, which triggers inflammation (Littlewood-Evans et al., 2016; Mills et al., 2021). Macrophage-derived extracellular succinate also activates GPR91 on neural stem cells (NSCs), which secrete prostaglandin E2 and scavenge extracellular succinate (Peruzzotti-Jametti et al., 2018). Hypoxia also increases succinylation (Gibson et al., 2015; Chen et al., 2017). Succinate-induced activation of GPR91 participates in ischemic injury by modulating processes such as cardiomyocyte hypertrophy and muscle remodeling (Aguiar et al., 2014; Wang et al., 2019). In terms of metabolic function, succinate accumulation induces mitochondrial respiration and changes the metabolic profile (Ehinger et al., 2016; Ives et al., 2020; Zhang et al., 2020; Avram et al., 2021). However, it is speculated that the role of intracellular succinate depends on its subcellular distribution.

Succinylation is a newly discovered and multienzyme-regulated post-translational modification that occurs in the cytoplasm. Succinylation can be non-enzymatic (regulated by succinyl-coenzyme A [CoA]) or enzymatic (Yang and Gibson, 2019). Succinate and succinyl-CoA can be converted into each other by succinyl-CoA synthetase and succinyl-CoA ligase, thus regulating succinylation. Improving succinate production by inactivation of succinate dehydrogenase induces hypersuccinylation by causing the accumulation of succinyl-CoA (Zhang et al., 2011; Li et al., 2015). Hypersuccinylation can lead to hypertrophic cardiomyopathy (Sadhukhan et al., 2016). Hypoxia also increases succinylation (Gibson et al., 2015; Chen et al., 2017). The regulation of succinylation is also associated with brain ischemic tolerance (Koronowski et al., 2018). For example, knockout of the desuccinylase sirtuin 5 (Sirt5) gene in mice makes them more susceptible to I/R injury compared with wild-type littermates. The succinylation of specific proteins, such as isocitrate dehydrogenase, in metabolic pathways alters their activity. Hence, further investigation on how succinylation modulates neurogenesis after I/R injury is needed.

[1]School of Medical Technology, Xuzhou Key Laboratory of Laboratory Diagnostics, Xuzhou Medical University, Xuzhou, Jiangsu Province, China; [2]College of Pharmacology, Xuzhou Medical University, Xuzhou, Jiangsu Province, China; [3]Research Center for Biochemistry and Molecular Biology and Jiangsu Key Laboratory of Brain Disease Bioinformation, Xuzhou Medical University, Xuzhou, Jiangsu Province, China; [4]School of Chinese Medicine, The University of Hong Kong, Hong Kong Special Administrative Region, China
*Correspondence to: Su-Hua Qi, PhD, suhuaqi@xzhmu.edu.cn.
https://orcid.org/0000-0003-0052-750X (Lin-Yan Huang); https://orcid.org/0000-0002-6507-2000 (Ju-Yun Ma); https://orcid.org/0000-0002-1807-0643 (Jin-Xiu Song); https://orcid.org/0000-0001-7745-3188 (Jing-Jing Xu); https://orcid.org/0000-0003-2857-9563 (Rui Hong); https://orcid.org/0000-0002-9840-0090 (Hai-Di Fan); https://orcid.org/0000-0002-0443-8769 (Heng Cai); https://orcid.org/0000-0003-0493-6407 (Wan Wang); Wang https://orcid.org/0000-0002-9173-504X (Yan-Ling Wang); https://orcid.org/0000-0002-2283-5880 (Zhao-Li Hu); https://orcid.org/0000-0002-4199-8095 (Jian-Gang Shen); https://orcid.org/0000-0002-1479-701X (Su-Hua Qi)
#These authors contributed equally to this work.

Funding: *This work was supported by the National Natural Science Foundation of China, No. 81671164 (to SHQ), the Natural Science Foundation of Jiangsu Province of China, No. BK20211348 (to SHQ), and Xuzhou Basic Research Program, No. KC21030 (to LYH).*
How to cite this article: *Huang LY, Ma JY, Song JX, Xu JJ, Hong R, Fan HD, Cai H, Wang W, Wang YL, Hu ZL, Shen JG, Qi SH (2023) Ischemic accumulation of succinate induces Cdc42 succinylation and inhibits neural stem cell proliferation after cerebral ischemia/reperfusion. Neural Regen Res 18(5):1040-1045.*

Here, we aimed to determine the level of succinate after cerebral I/R injury and the effects of the altered metabolite levels of succinate on neurogenesis, such as NSC proliferation. We also investigated the mechanism by which succinate regulates NSC proliferation to affect the outcome of ischemic stroke.

Methods

Establishment of a rat model of ischemia/reperfusion injury

All animal experiments were approved by the Laboratory Animal Ethics Management Committee of Xuzhou Medical University, Xuzhou, China (approval No. 201904W047) on April 15, 2019, and were performed in accordance with the guidelines of the animal facility of Xuzhou Medical University.

All rats were kept under a constant temperature 23 ± 2°C and a 12-hour light/dark cycle. They were fed with a commercially available normal rat diet and tap water *ad libitum*. To avoid the influence of estrogen on cerebral cardiovascular disease (Prabakaran et al., 2022), only male rats were chosen to establish the middle cerebral artery occlusion (MCAO) model and to observe the effects of succinate. We used 24 adult male Sprague-Dawley rats (Shanghai Institute for Biomedical and Pharmaceutical Technologies, Shanghai, China, license No. SCXK (Hu) 2018-0006) that were specific-pathogen-free, 5–8 weeks old, and weighed 200 to 250 g in this study. The MCAO model was induced using an established method described previously (Hu et al., 2020). Briefly, rats were anesthetized with 4% isoflurane (RWD Life Science Co., Ltd., Shenzhen, China) and were maintained at 2% isoflurane via inhalation. Then the common, external, and internal carotid arteries were exposed through a ventral midline incision. A silicone-coated 4-0 monofilament nylon suture with a rounded tip was inserted into the right common carotid artery and was advanced until it occluded the middle cerebral artery. Then the anesthesia was reversed. After 1 hour of occlusion, the rat was reanesthetized and the nylon suture was withdrawn. Rectal temperature was maintained around 37°C throughout the surgical procedure using a feedback-regulated heating system (Zhike Company, Zhengzhou, China).

To measure succinate levels, 12 rats were randomly divided into sham and MCAO groups (n = 6/group). To measure diethyl succinate (DS) levels, an additional 12 rats were randomly divided into MCAO and MCAO + DS groups (n = 6/group). DS (800 mg/kg, MilliporeSigma, Burlington, MA, USA) was injected intraperitoneally 2 hours after ischemia, and then reperfusion was performed for 24 hours. Detailed information about the study design is provided in **Additional Figure 1**.

Cell culture

Primary neural stem cell culture

One pregnant rat (E14–19, Shanghai Institute of Planned Parenthood Research-Bk Lab Animal Co., Ltd., Shanghai, China) was anesthetized by inhalation of 97.5% ether for 5 minutes (Sinopharm Chemical Reagent Co., Ltd., Shanghai, China) and decapitated. The rat was disinfected with 75% alcohol and the fetuses were removed from the rat. One rat fetus was rinsed with ultrapure water containing 1% penicillin/streptomycin and placed in a petri dish filled with precooled high-glucose Dulbecco's Modified Eagle Medium (DMEM) (Cat# KGM12800-500, KeyGEN BioTECH, Nanjing, China). The cortex and hippocampus were separated from the rest of the brain under a research stereomicroscope (SZX16, Olympus, Tokyo, Japan), chopped into small pieces, and transferred into a 50-mL sterile tube. After centrifugation at 1000 r/min for 10 minutes, the pellet was mixed with trypsin (Beyotime Biotechnology, Shanghai, China) and digested in a 37 °C water bath for 15–25 minutes with gentle shaking. After filtration, DMEM with 1% penicillin/streptomycin was used to stop digestion. The pellet was resuspended in NSC basal medium (100 mL DMEM [KeyGEN BioTECH], 2 mL 2% B-27 [Thermo Fisher Scientific, Waltham, MA, USA], 1 mg epidermal growth factor [MedChemExpress LLC, Monmouth Junction, NJ, USA], and 1 mg fibroblast growth factor [MedChemExpress LLC]) and transferred into a culture flask. After 24 hours, the medium was collected and centrifuged. Half of the supernatant was refreshed with new medium every other day. On the 11th day, the resultant neurospheres were collected and washed with phosphate-buffered saline on ice. The neurospheres were digested with trypsin and the cells were cultured in NSC complete medium (NSC basal medium with 20% fetal bovine serum [FBS; Thermo Fisher Scientific]) and filtered through a 200-μm nylon mesh (Beijing Solarbio Science & Technology Co., Ltd., Beijing, China) to obtain the NSC suspension. Primary NSCs were cultured to detect the G protein-coupled succinate receptor GPR91 and intracellular succinate levels after oxygen-glucose deprivation/reoxygenation (OGD/R) treatment.

Cell culture of the neural stem cell line C17.2

The multipotent mouse NSC line C17.2 (RRID: CVCL4511) was provided by the School of Chinese Medicine, Li Ka Shing Faculty of Medicine, The University of Hong Kong, China. C17.2 cells were cultured in high-glucose DMEM (Cat# KGM12800-500, KeyGEN BioTECH) supplemented with 10% FBS at 37°C in humidified incubators with 5% carbon dioxide, as previously described (Hu et al., 2020).

Oxygen-glucose deprivation/reoxygenation treatment

To mimic ischemic stroke conditions *in vitro*, primary NSCs and C17.2 cells were subjected to OGD/R treatment. In brief, OGD/R experiments were performed in a humidified incubator (ESCO Life Sciences Group, Bintan Island, Indonesia) at 37°C with 90% nitrogen, 5% hydrogen, and 5% carbon dioxide, and culture medium was replaced with glucose-free DMEM (Cat# 11966025, Thermo Fisher Scientific). After 6 hours, the culture medium was replaced with complete medium (high-glucose DMEM [Cat# KGM12800-500, KeyGEN BioTECH] containing 10% FBS), and the cells were left to recover for 24 hours in a regular incubator. Control cells were incubated in complete medium under normoxia for the same duration.

Measurement of succinate by liquid chromatography–tandem mass spectrometry analysis

Blood was collected via the abdominal aorta of rats in the sham and MCAO groups after anesthesia by peritoneal injection of 2% pentobarbital sodium (Cat# Y0002194, MilliporeSigma). Serum was separated from whole blood by centrifugation for 10 minutes at 2500 × *g* for use in the succinate assay. The ischemic cortices and hippocampi were collected 24 hours after reperfusion and homogenized. After centrifugation at 2500 × *g* for 10 minutes, the supernatant was aspirated for use in the succinate assay. Before detection, 50-μL aliquots of the samples were mixed with 195 μL methanol containing 10 μM succinic acid-2,2,3,3-d4 (Cat# 293075, MilliporeSigma) for 2 minutes and this mixture was centrifuged for 10 minutes at 12,000 × *g*. Then, 150 μL of the mixture was collected for liquid chromatography-tandem mass spectrometry (LC-MS/MS). The NSCs subjected to OGD/R were treated with methanol to extract proteins and metabolites and then sonicated. The extraction mixture was combined with succinic acid-2,2,3,3-d4 and centrifuged at 12,000 × *g* for 10 minutes. The supernatant was taken for LC-MS/MS using 10 μM succinic acid-2,2,3,3-d4 as the internal standard.

All samples were analyzed in multiple reaction monitoring mode using an ultra-performance liquid chromatography/triple quadrupole system (Waters Corp., Milford, MA, USA) with an electrospray ionization probe and an Acquity UPLC BEH C18 column (2.1 × 50 mm; 1.7 μm; Waters Corp.). The mobile phase was maintained at a flow rate of 0.4 mL/min and contained 0.1% (v/v) formic acid water solution (buffer A) and 0.1% (v/v) formic acid acetonitrile solution (buffer B). Succinic acid was separated using a gradient of 10% buffer B for 0.2 minutes, 10% buffer B to 80% buffer B for 1.8 minutes, 80% buffer B for 0.5 minutes, and 80% buffer B to 10% buffer B for 0.5 minutes, followed by a hold with 10% buffer B for 1.5 minutes. The temperature of the column was maintained at 40°C. The electrospray ionization source was set in negative ionization mode. Quantification was performed using multiple reaction monitoring with m/z 117 to 73 for succinic acid quantification, m/z 117 to 98 for succinic acid identification, m/z 121 to 77 for internal standard quantification, and m/z 121 to 102 for internal standard identification. The optimal MS parameters included capillary voltage of 1.16 kV, cone voltage of 24 V, collision voltage of 12 V, source temperature of 150°C, and desolvation temperature of 600°C. The desolvation flow rate was 600 L/h.

2,3,5-Triphenyltetrazolium chloride staining

2,3,5-Triphenyltetrazolium chloride staining is commonly used to identify hypoxic brain tissue and to define the size of cerebral infarctions (Chen et al., 2020). At 24 hours after reperfusion, rats were sacrificed by peritoneal injection of 2% pentobarbital sodium and the brains were quickly dissected. The harvested brains were placed at –20°C for 30 minutes, cut into 2-mm-thick slices, and stained with 2% 2,3,5-triphenyltetrazolium chloride (A610558, Sangon Biotech, Shanghai, China) at 37°C for 25 minutes. The brain slices were fixed in 4% paraformaldehyde solution and photographed with a digital camera (EOS 2000D, Canon, Tokyo, Japan). The infarct area in each brain slice was measured using Image J Fiji (National Institutes of Health, Bethesda, MD, USA) (Schindelin et al., 2012). The relative infarct percentage was calculated using the following formula: Infarct percentage = (non-infarct hemisphere area – infarct hemisphere non-infarct area)/non-infarct hemisphere area × 100. An independent pathologist evaluated 2,3,5-triphenyltetrazolium chloride staining.

Evaluation of neurobehavioral function

The modified neurological severity score (mNSS) was determined 1 day prior to and 1 day after MCAO and was performed by researchers blinded to the experimental design. The mNSS score includes exercise and sensory tests and reflex evaluation. The mNSS ranges from 0 to 18. A higher score indicates more severe deficits (Chen et al., 2001).

Cell viability assay

C17.2 cells were plated in 96-well cell culture plates at 5 × 10^3 cells/well and incubated for 24 hours. To compare the effects of succinic acid and DS on cell proliferation, we added 0.5, 1, 2, 5, or 10 mM DS or 100, 200, 400, or 1000 μM succinic acid to the cells. ML141 is a potent and selective inhibitor of Cdc42 (Chaker et al., 2018). To confirm if DS inhibits C17.2 proliferation by inhibition of Cdc42 activity, we compared the effects of DS and ML141. We added DS (1, 5, or 10 mM) or ML141 (1, 5, or 10 mM) to 5 × 10^3 C17.2 cells/well after 24 hours of incubation. After a further 48 hours, cell viability was determined using the Cell Counting Kit-8 (CCK8) (Cat# C0037, Beyotime Biotechnology) in accordance with the manufacturer's instructions. The absorbance (A) value was measured at 450 nm using a microplate reader (Bio-Rad Laboratories, Hercules, CA, USA). The A value of a well without cells was recorded as A_{blank}. The percent cell viability was calculated using the following formula: Cell viability = $(A_{treatment} - A_{blank})/(A_{control} - A_{blank}) \times 100$.

Immunofluorescence staining

To visualize the distribution of succinate receptor GPR91 on primary NSCs (that stain positive for nestin), we performed dual immunofluorescence staining. Briefly, primary NSCs were seeded on a coverslip and fixed with 4% paraformaldehyde. The coverslip was washed with phosphate-buffered saline,

and the slides were treated with phosphate-buffered saline containing 0.1% Triton X-100 and 5% bovine serum albumin (Cat# VIC018, Vicmed, Xuzhou, China) for 1 hour. The slides were incubated with the following primary antibodies at 4°C overnight: rabbit anti-GPR91 polyclonal antibody (1:1000; Cat# 223051, United States Biological, Salem, MA, USA) and mouse anti-nestin monoclonal antibody (1:1000; Cat# NBP1-92717, RRID: AB_11020601, Novus Biologicals, Littleton, CO, USA). Then, the slides were incubated with goat anti-mouse Alexa Fluor 488-labeled secondary antibody (1:1000; Cat# A11001, RRID: AB_2534069, Thermo Fisher Scientific) or goat anti-rabbit Cy3-labelled secondary antibody (1:1000; Cat# AS007, RRID: AB_2769089, ABclonal, Woburn, MA, USA) at room temperature for 1 hour. Representative images were obtained using a laser-scanning confocal microscope (TCS SP5, Leica, Wetzlar, Germany). We used 4′,6-diamidino-2-phenylindole (10 mg/mL; Cat# KGA215-10, KeyGen BioTECH) to label cell nuclei.

Western blot assay

We measured the levels of Cdc42 and other proteins by western blot to investigate the effect of DS on NSC proliferation. Western blot was performed as previously described (Huang et al., 2014). Briefly, C17.2 cells were lysed with radio immunoprecipitation assay lysis buffer containing a protease inhibitor cocktail (Merck, Darmstadt, Germany). Proteins were separated by 10% sodium dodecyl sulfate-polyacrylamide gel electrophoresis and were transferred to polyvinylidene fluoride membranes (MilliporeSigma). The membranes were blocked in 5% non-fat dry milk diluted with Tris-buffered saline containing 0.1% Tween 20 (20 mM Tris-HCl, 150 mM NaCl pH 7.5, 0.1% Tween 20) at room temperature for 1 hour. The membranes were incubated with primary antibody at 4 °C overnight: rabbit anti-GPR91 polyclonal antibody (1:1000; Cat# 223051, United States Biological), rabbit anti-SIRT5 monoclonal antibody (1:1000; Cat# 8782, RRID: AB_2716763, Cell Signaling Technology, Danvers, MA, USA), rabbit anti-Cdc42 monoclonal antibody (1:1000; Cat# ab187643, RRID: AB_2818943, Abcam, Cambridge, UK), or rabbit anti-succinyllysine polyclonal antibody (1:1000; Cat# PTM-401, RRID: AB_2687628, PTM Biolabs, Hangzhou, China). Then, the membranes were incubated for 1 hour at room temperature with anti-rabbit IgG conjugated to horseradish peroxidase (1:1000; Cat# SA00001-2, RRID: AB_2722565, Proteintech, Rosemont, IL, USA) or anti-mouse IgG conjugated to horseradish peroxidase (1:1000; Cat# SA00001-1, RRID: AB_2722565, Proteintech). The loading controls were rabbit anti-β-actin monoclonal antibody (1:1000; Cat# 4970, RRID: AB_2223172, Cell Signaling Technology), mouse α-tubulin monoclonal antibody (1:1000; Cat# 66031-1-Ig, RRID: AB_11042766, Proteintech), or mouse glyceraldehyde 3-phosphate dehydrogenase (GAPDH) monoclonal antibody (1:1000; Cat# 60004-1-Ig, RRID: AB_2107436, Proteintech). All bands were detected with Pierce ECL Western Blotting Substrate (Thermo Fisher Scientific).

Measurement of Cdc42 GTPase activity

Cdc42 GTPase activity was performed using the Rac1/Cdc42 Activation Assay Kit (Cat# 17-441, MilliporeSigma), which pulls down GTP-Cdc42 using its downstream effector p21-activated protein kinase (PAK1). Briefly, C17.2 cells were lysed to collect the supernatant and incubated with PAK1-PBD agarose beads for 12 hours at 4°C. The agarose beads were washed three times with lysis buffer, resuspended in Laemmli buffer (Vicmed), and boiled for 5 minutes. The supernatant was collected for sodium dodecyl sulfate-polyacrylamide gel electrophoresis and subsequent immunoblot. The blots were probed with anti-Cdc42 antibody to detect the levels of GTP-Cdc42 and total Cdc42.

Co-immunoprecipitation of Cdc42 succinylation

Because succinylation is a newly identified post-translational modification (Yang and Gibson, 2019), we hypothesized that succinate might affect the downstream target of GPR91, Cdc42, by succinylation. Therefore, we measured Cdc42 GTPase activity and succinylation by coimmunoprecipitation. C17.2 cells were treated with immunoprecipitation lysis buffer (Cat# 87787, Thermo Fisher Scientific) on ice for 15 minutes. The cell lysates were centrifuged, and the cellular extracts were collected. Succinyllysine antibody or Cdc42 antibody were incubated with the cellular extracts at 4°C overnight. Protein G or protein A agarose beads (Thermo Fisher Scientific) were incubated with the cellular extracts for 4 hours. Then, the beads were washed twice with immunoprecipitation lysis buffer, and the proteins were eluted in 1× Laemmli buffer (50 mM Tris-HCl pH 6.8, 1% sodium dodecyl sulfate, 6% glycerol, 1% β-mercaptoethanol, and 0.004% bromophenol blue). Proteins were separated by sodium dodecyl sulfate-polyacrylamide gel electrophoresis and analyzed by immunoblotting with Cdc42 antibody and succinyllysine antibody.

Transfection of siRNA

C17.2 cells with or without OGD/R treatment were incubated in 0.6 mL/well antibiotic-free DMEM supplemented with 10% FBS and 2 mM L-glutamine for 2 hours. Then, we prepared Sirt5 siRNA (Sangon, Shanghai, China), Gpr91 siRNA (Sangon), or negative control siRNA (Sangon) in Lipofectamine 3000 (Thermo Fisher Scientific) and Opti-MEM I (Cat# 31985070, Thermo Fisher Scientific). Next, C17.2 cells were pretreated with Sirt5 siRNA, Gpr91 siRNA, or negative control siRNA for 6 hours in accordance with the manufacturer's instructions.

Statistical analysis

Statistical analysis was performed using GraphPad Prism 8.0.2 software (GraphPad Software, San Diego, CA, USA; www.graphpad.com). All experimental data are expressed as the mean ± standard deviation (SD). The comparisons of succinate (*in vivo*) were analyzed by two-way analysis of variance followed by Tukey's *post hoc* tests. The comparisons of infarct volume, neurobehavioral scores, and GPR91 and SIRT5 expression were analyzed by unpaired *t*-tests. The comparisons of succinate (*in vitro*) were analyzed with repeated measures analysis of variance followed by Dunnett's *post hoc* tests. The data for CCK8 were analyzed by one-way analysis of variance followed by Dunnett's post hoc tests or Tukey's *post hoc* tests. The comparisons of Cdc42 levels were analyzed by one-way or two-way analysis of variance followed by Tukey's *post hoc* tests. Values were considered statistically significant when $P < 0.05$.

Results

Abnormal levels of succinate accumulate after cerebral ischemia/reperfusion injury

To determine whether succinate accumulates in the tissues of rats after I/R injury, we used LC-MS/MS technology to detect the level of succinate in different rat tissues in the sham and MCAO groups. Our data showed that succinate levels were higher in the serum ($P < 0.05$), cortex ($P < 0.01$), and hippocampus ($P < 0.01$) in the MCAO group compared with that in the sham group (**Figure 1A**). To test the level of succinate in NSCs after I/R, we established a stroke model in primary NSCs using OGD/R and detected intracellular succinate by LC-MS/MS. We found that the basal concentration of intracellular succinate was 0.36 ± 0.08 μM, and after 2 hours of OGD, succinate increased to 3.28 ± 0.19 μM ($P < 0.01$, *vs.* sham group). The succinate concentration then decreased to the basal level immediately after 10 minutes of reoxygenation, and this basal level was maintained for a further 24 hours (**Figure 1B**).

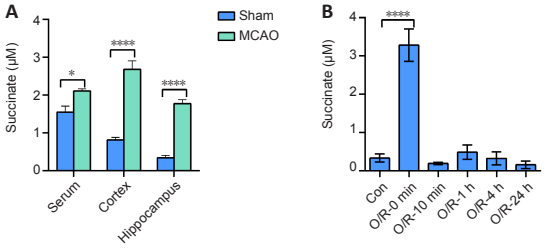

Figure 1 | **Succinate accumulates after cerebral ischemia/reperfusion *in vivo* and *in vitro*.**

(A) Succinate accumulates in serum, cortex, and hippocampus of middle cerebral artery occlusion (MCAO) rats ($n = 6$ rats/group). (B) Levels of intracellular succinate in neural stem cells subjected to oxygen-glucose deprivation and reperfusion (O/R). Each experiment was repeated three times. Data are expressed as the mean ± SD and were analyzed by (A) two-way analysis of variance followed by Tukey's *post hoc* test or (B) repeated measures analysis of variance followed by Dunnett's *post hoc* test. *$P < 0.05$, ****$P < 0.0001$.

Succinate inhibits NSC proliferation under physiological and oxygen-glucose deprivation/reoxygenation conditions.

Cell viability also corresponds to proliferation ability. Hence, we used the CCK8 assay to detect the effects of succinate on NSC proliferation. We chose DS, a derivative of succinate, for *in vitro* experiments, as previously reported (Harber et al., 2020). There was no effect on NSC proliferation at 100, 200, 400, or 1000 μM succinic acid under physiological or OGD/R conditions (**Additional Figure 2**). However, we observed that 0.5–10 mM DS inhibited C17.2 cell proliferation in a dose-dependent manner under physiological and OGD/R conditions (**Figure 2A** and **B**).

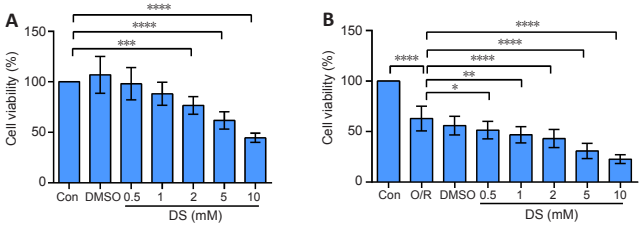

Figure 2 | **Succinate inhibits neural stem cell proliferation in a concentration-dependent manner.**

(A, B) The viability of C17.2 cells after diethyl succinate treatment under (A) physiological and (B) oxygen-glucose deprivation and reperfusion (O/R) conditions. Data are expressed as the mean ± SD. Each experiment was repeated three times. *$P < 0.05$, **$P < 0.01$, ***$P < 0.001$, ****$P < 0.0001$ (one-way analysis of variance followed by Dunnett's *post hoc* test). Con: Negative control; DMSO: dimethyl sulfoxide; DS: diethyl succinate.

Administration of succinate aggravates cerebral ischemia/reperfusion injury *in vivo*

Figure 3A shows the experimental design. Rats in the MCAO + DS group had a larger infarct volume ($P < 0.05$; **Figure 3B** and **C**) and higher mNSS ($P < 0.01$; **Figure 3D**) than rats in the MCAO group, demonstrating that succinate accumulation aggravated I/R injury.

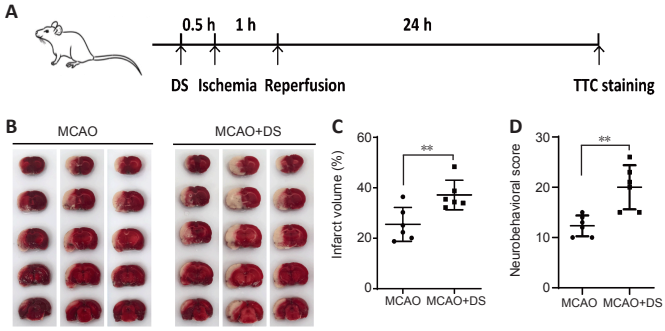

Figure 3 | Succinate administration aggravates cerebral ischemia/reperfusion injury.
(A) The middle cerebral artery occlusion (MCAO) rat model and diethyl succinate (DS) administration. (B) 2,3,5-Triphenyltetrazolium chloride (TTC) staining shows that DS increases infarct volume after cerebral ischemia/reperfusion injury. The infarcted brain tissue of the MCAO rat model appeared white, whereas the normal brain tissue appeared red. (C, D) Quantitative results of (C) infarct volume and (D) neurobehavioral scores. Data are expressed as the mean ± SD (n = 6 rats/group). $^{**}P < 0.01$ (unpaired t-test).

Succinate receptor GPR91 is unnecessary for inhibition of C17.2 cell proliferation by diethyl succinate

We confirmed the expression of the succinate receptor GPR91 in primary NSCs. The immunofluorescence assay showed that GPR91 and nestin colocalized in primary NSCs (**Figure 4A**). However, GPR91 expression was unaffected after OGD/R or DS treatment (**Figure 4B** and **C**). Western blot results showed that GPR91 expression was significantly increased in C17.2 cells after OGD/R compared with that in the negative control group (**Figure 4D**). Although DS inhibited cell proliferation, Gpr91 knockdown did not reverse cell proliferation inhibited by DS under physiological or OGD/R conditions (both $P > 0.05$; **Figure 4E** and **F**). Thus, GPR91 is not necessary for inhibition of C17.2 proliferation by DS.

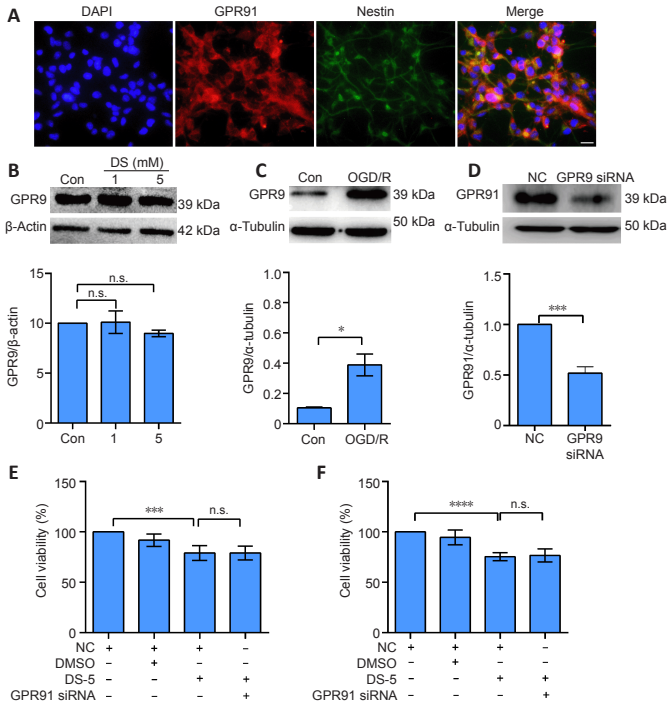

Figure 4 | Succinate receptor G protein-coupled receptor 91 is unnecessary for diethyl succinate-mediated inhibition of C17.2 cell proliferation after oxygen-glucose deprivation/reoxygenation.
(A) Dual immunofluorescence analysis of G protein-coupled receptor 91 (GPR91; red) and nestin (green, Alexa Fluor 488) in primary neural stem cells. GPR91 and nestin colocalize (shown in yellow in the merge image) in primary neural stem cells. Scale bar: 50 μm. (B) Quantitative results of GPR91 expression in C17.2 cells treated with 1 or 5 mM diethyl succinate (DS) under physiological conditions. (C) Quantitative results of GPR91 expression in C17.2 cells under oxygen-glucose deprivation/reoxygenation. (D) Quantitative results of GPR91 expression in C17.2 cells transfected with Gpr91 siRNA. (E) The effects of Gpr91 siRNA transfection on C17.2 cell proliferation inhibited by DS under physiological conditions, as assessed by the Cell Counting Kit-8 (Beyotime Biotechnology). (F) The effects of Gpr91 siRNA transfection on C17.2 cell proliferation inhibited by DS under oxygen-glucose deprivation/reoxygenation conditions, as assessed by the Cell Counting Kit-8 (Beyotime Biotechnology). Each experiment (except for dual immunofluorescence analysis) was repeated three times. Data are expressed as the mean ± SD and were analyzed by one-way analysis of variance followed by (B) Dunnett's or (E, F) Tukey's *post hoc* test or by (C, D) unpaired t-test. $^{*}P < 0.05$, $^{***}P < 0.01$, $^{****}P < 0.0001$. Con: Negative control; DAPI: 4′,6-diamidino-2-phenylindole; DMSO: dimethyl sulfoxide; DS-5: 5 mM diethyl succinate; NC: negative control; n.s.: no significance.

Succinate inhibits GTP-Cdc42 activity by increasing Cdc42 succinylation *in vitro*

Total Cdc42 levels did not change after OGD/R treatment or DS and OGD/R combined (**Figure 5A** and **B**). DS treatment during OGD/R significantly inhibited GTP-Cdc42 activity (**Figure 5A** and **C**) and increased Cdc42 succinylation (**Figure 5D**). To determine whether the succinylation of Cdc42 affects its GTPase activity, we performed Sirt5 siRNA transfection to increase total succinylation levels in C17.2 cells. Cdc42 succinylation was increased in C17.2 cells transfected with Sirt5 siRNA, whereas Cdc42 GTPase activity was decreased compared with the negative control group (**Figure 5E** and **F**). Thus, increasing Cdc42 succinylation might contribute to inhibition of Cdc42 GTPase activity by DS.

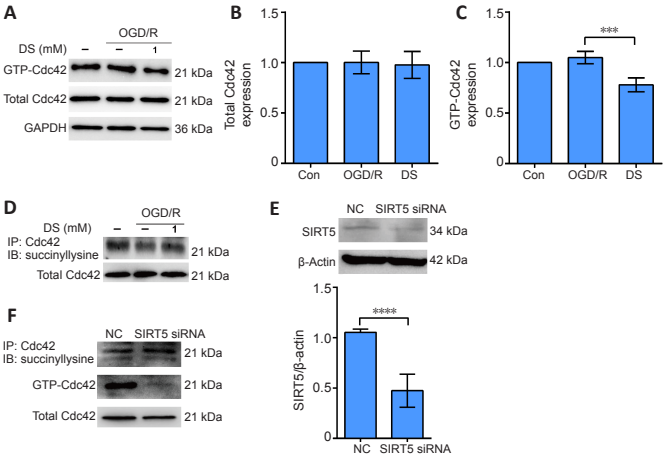

Figure 5 | Diethyl succinate inhibits GTP-Cdc42 activity by increasing Cdc42 succinylation in C17.2 cells.
(A) Cdc42 GTPase activity using a Rac1/Cdc42 activation assay. (B, C) Quantitative results of the (B) total Cdc42 and (C) GTP-Cdc42 levels in C17.2 cells treated with diethyl succinate (DS). (D) Cdc42 succinylation in neural stem cells was assayed by coimmunoprecipitation. (E) The effects of sirtuin 5 (Sirt5) siRNA transfection in C17.2 cells were detected by western blot. The experiment was repeated three times. (F) The increase in Cdc42 succinylation by Sirt5 siRNA transfection represses the level of GTP-Cdc42. Data are expressed as the mean ± SD and were analyzed by one-way analysis of variance followed by (B, C) Tukey's *post hoc* test or (F) unpaired t-test. $^{***}P < 0.001$, $^{****}P < 0.0001$. Con: Negative control; GAPDH: glyceraldehyde 3-phosphate dehydrogenase; IB: immunoblot; IP: immunoprecipitation NC: negative control; OGD/R: oxygen–glucose deprivation/reoxygenation.

Suppression of Cdc42 GTPase activity inhibits C17.2 proliferation after oxygen-glucose deprivation/reoxygenation

The CCK8 assay results showed that OGD/R reduced C17.2 cell proliferation compared with that in the negative control group ($P < 0.01$; **Figure 6**). DS (1, 5, and 10 mM) inhibited C17.2 proliferation compared with that in the OGD/R group ($P < 0.05$, $P < 0.01$, and $P < 0.01$, respectively; **Figure 6**). ML141 (1, 5, and 10 mM) inhibited cell proliferation compared with that in the OGD/R group ($P < 0.01$, $P < 0.01$, and $P < 0.0001$, respectively; **Figure 6**). Thus, under OGD/R, C17.2 cell proliferation inhibited by DS might be caused by suppression of Cdc42 activity.

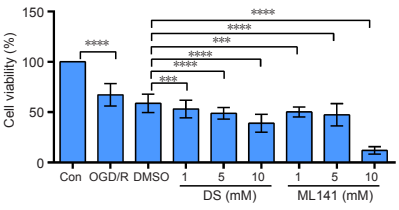

Figure 6 | Inhibition of Cdc42 GTPase activity reduces C17.2 cell proliferation under oxygen-glucose deprivation/reperfusion conditions.
The effects of diethyl succinate (DS) and ML141 on C17.2 cell proliferation under oxygen-glucose deprivation/reperfusion (OGD/R) conditions were detected with the Cell Counting Kit-8. The experiment was repeated three times. Data are expressed as the mean ± SD and were analyzed by one-way analysis of variance followed by Dunnett's *post hoc* test. $^{***}P < 0.001$, $^{****}P < 0.0001$. Con: Negative control; DMSO: dimethyl sulfoxide.

Discussion

Our study demonstrates that abundant succinate is present in the serum, cortex, and hippocampus of MCAO rats. Succinate increases Cdc42 succinylation, which represses Cdc42 GTPase activity and, in turn, inhibits NSC proliferation after cerebral I/R injury. Our data expand the knowledge of ischemic accumulation of succinate causing cerebral I/R injury in NSCs.

Under physiological conditions, circulating levels of succinate range from 2 to 20 μM, and succinate levels increase exponentially under pathological conditions such as I/R injury following myocardial infarction (Kohlhauer et al., 2018). Ischemic accumulation of succinate causes reperfusion injury by release of mitochondrial reactive oxygen species (Chouchani et al., 2014). We detected elevated levels of succinate in serum and brain tissue (cortex and hippocampus) in the rat MCAO model, which warranted exploration of the effects of tissue-derived succinate on neurological function.

Because NSCs produce a comparable amount of succinate after OGD compared to physiological condition, we chose DS, a membrane-permeable succinate that increases intracellular succinate (Tannahill et al., 2013; Li et al., 2017), to study the effects of intracellular succinate on NSCs. As expected, DS inhibited NSC proliferation under OGD/R conditions. Furthermore, DS increased infarct volumes and neurobehavioral scores in the MCAO rat model, showing that DS increases the severity of the MCAO model and that inhibition of proliferation by DS is the dominant role in neural damage after I/R injury.

Succinate may function as a metabolic or non-metabolic molecule, depending on its distribution (Grimolizzi and Arranz, 2018). In mitochondria, succinate plays a crucial role in metabolism and operates in both anabolic and catabolic pathways (Tannahill et al., 2013; Kelly and O'Neill, 2015). In the cytosol, elevated cytosolic succinate levels may increase protein post-translational modifications by addition of succinyl groups to lysine residues (Xie et al., 2012; Park et al., 2013). Additionally, succinate may be released to the extracellular space through plasma membrane transporters of the sodium sulfate/carboxylate cotransporter family (Willmes and Birkenfeld, 2013). Extracellular succinate affects the surrounding microenvironment by GPR91-mediated signal transduction (Rubic et al., 2008). Although we did not test the effect of succinic acid (extracellular succinate) on NSC proliferation, we confirmed that the effect of DS (intracellular succinate) on NSC proliferation was not related to GPR91.

Many cellular processes are controlled by small GTPases of the Rho family, including RhoA, Rac1, and Cdc42 (Nobes and Hall, 1995), which each possess different functions. Cdc42 activation and I/R injury are related (Yang et al., 2019). Cdc42 is implicated in the regulation of a variety of biological activities in the nervous system, such as cell signaling, cytoskeleton organization, establishment of neuron polarity, and regulation of cell morphology, motility, and cell cycle progression (Etienne-Manneville and Hall, 2003). The effector proteins recognize the activated form of Cdc42 and induce conformational changes in Cdc42 (especially changes to the switch I and switch II loops), which are critical for activation of the subsequent signaling pathway. GPR91 is responsible for the biological functions of succinate beyond energy production (de Castro Fonseca et al., 2016). We speculated that DS might influence the function of GPR91, as GPR91 can bind G proteins such as Gαi or Gq. Gαi activation causes the inactivation of Cdc42 (Kedziora et al., 2016; Reinhard et al., 2017; Traulsen et al., 2021). Our results demonstrate that DS did not alter total Cdc42 levels after OGD/R exposure, but DS did reduce Cdc42 GTPase activity in NSCs.

Cdc42 activity is also regulated by its various post-translational modifications, such as monophosphate adenylation, phosphorylation, glycosylation, and lysine succinylation. Lysine succinylation is regulated by SIRT5 (Zhang et al., 2011; Park et al., 2013) and is an important regulator of cellular processes, such as metabolism, inflammation, and microbial infection (Park et al., 2013; Ren et al., 2018; Yang and Gibson, 2019). Succinylation regulated by SIRT5 plays a diverse role in protein activity. The inhibition of mitochondrial antiviral-signaling protein activation by SIRT5-induced desuccinylation causes impairment of type I interferon production and subsequent impairment of antiviral gene expression (Liu et al., 2020). However, Sirt5 knockdown increases succinylation and subsequent activity of acyl-CoA oxidase 1 in hepatocellular carcinoma (Chen et al., 2018). Previous reports have not determined whether Cdc42 succinylation is also involved in the regulation of Cdc42 activity. Thus, to confirm whether Cdc42 succinylation affects Cdc42 GTPase activity, we increased Cdc42 succinylation by Sirt5 knockdown and found that Cdc42 activity was repressed. As expected, decreased Cdc42 activity using the Cdc42 inhibitor ML141 also inhibited NSC proliferation in a comparable manner to DS. Hence, our data support the idea that DS-induced Cdc42 succinylation affects Cdc42 GTPase activity, which causes the inhibition of NSC proliferation after cerebral I/R injury.

There were some limitations to our study. We did not explore the specific sites of succinylation in Cdc42 that were triggered by DS after OGD/R treatment. We also did not explore the effects of DS on migration and differentiation, which are other factors besides proliferation that relate to neurogenesis, but this could be investigated in future studies.

Our research expands the knowledge of how ischemic accumulation of succinate causes reperfusion injury. Unexpectedly, we found that succinate inhibits NSC proliferation by succinylation of Cdc42, which is harmful for neural recovery after I/R injury. Our data support the idea that modulation of succinate levels or Cdc42 activity might be a potential therapeutic target for I/R injury.

Acknowledgments: *We thank Dr. Yuan Zhou from Xuzhou Medical University for the assistance on the measurement of succinate by liquid chromatography tandem mass spectrometry. We also thank the technical assistance of Public Experimental Research Center of Xuzhou Medical University. We also thanked Professor Jian-Gang Shen (School of Chinese Medicine, Li Ka Shing Faculty of Medicine, The University of Hong Kong, China) for providing C17.2 cells.*
Author contributions: *Study design and coordination: LYH, SHQ; experiment implementation, and data collection and analysis: JYM, JXS; manuscript drafting: JJX, RH, HDF, HC, WW, YLW, ZLH, JGS. All authors read and approved the final manuscript.*
Conflicts of interest: *The authors declare that they have no competing interests.*
Author statement: *This paper has been posted as a preprint on Research Square with doi:10.21203/rs.3.rs-871703/v1, which is available from: https://assets.researchsquare.com/files/rs-871703/v1/af016698-2b0b-4362-a8a5-99f1d408be50.pdf?c=1634303100.*
Availability of data and materials: *All data generated or analyzed during this study are included in this published article and its supplementary information files.*

Additional files:
Additional Figure 1: *Experimental design and timeline.*
Additional Figure 2: *Different concentrations of succinic acid (SA) have no effect on C17.2 cell proliferation.*

References

Aguiar CJ, Rocha-Franco JA, Sousa PA, Santos AK, Ladeira M, Rocha-Resende C, Ladeira LO, Resende RR, Botoni FA, Barrouin Melo M, Lima CX, Carballido JM, Cunha TM, Menezes GB, Guatimosim S, Leite MF (2014) Succinate causes pathological cardiomyocyte hypertrophy through GPR91 activation. Cell Commun Signal 12:78.

Avram VF, Chamkha I, Åsander-Frostner E, Ehinger JK, Timar RZ, Hansson MJ, Muntean DM, Elmér E (2021) Cell-permeable succinate rescues mitochondrial respiration in cellular models of statin toxicity. Int J Mol Sci 22:424.

Chaker D, Mouawad C, Azar A, Quilliot D, Achkar I, Fajloun Z, Makdissy N (2018) Inhibition of the RhoGTPase Cdc42 by ML141 enhances hepatocyte differentiation from human adipose-derived mesenchymal stem cells via the Wnt5a/PI3K/miR-122 pathway: impact of the age of the donor. Stem Cell Res Ther 9:167.

Chen H, Xu H, Potash S, Starkov A, Belousov VV, Bilan DS, Denton TT, Gibson GE (2017) Mild metabolic perturbations alter succinylation of mitochondrial proteins. J Neurosci Res 95:2244-2252.

Chen H, Guan B, Wang B, Pu H, Bai X, Chen X, Liu J, Li C, Qiu J, Yang D, Liu K, Wang Q, Qi S, Shen J (2020) Glycyrrhizin prevents hemorrhagic transformation and improves neurological outcome in ischemic stroke with delayed thrombolysis through targeting peroxynitrite-mediated HMGB1 signaling. Transl Stroke Res 11:967-982.

Chen J, Sanberg PR, Li Y, Wang L, Lu M, Willing AE, Sanchez-Ramos J, Chopp M (2001) Intravenous administration of human umbilical cord blood reduces behavioral deficits after stroke in rats. Stroke 32:2682-2688.

Chen XF, Tian MX, Sun RQ, Zhang ML, Zhou LS, Jin L, Chen LL, Zhou WJ, Duan KL, Chen YJ, Gao C, Cheng ZL, Wang F, Zhang JY, Sun YP, Yu HX, Zhao YZ, Yang Y, Liu WR, Shi YH, et al. (2018) SIRT5 inhibits peroxisomal ACOX1 to prevent oxidative damage and is downregulated in liver cancer. EMBO Rep 19:e45124.

Chouchani ET, Pell VR, Gaude E, Aksentijević D, Sundier SY, Robb EL, Logan A, Nadtochiy SM, Ord ENJ, Smith AC, Eyassu F, Shirley R, Hu CH, Dare AJ, James AM, Rogatti S, Hartley RC, Eaton S, Costa ASH, Brookes PS, et al. (2014) Ischaemic accumulation of succinate controls reperfusion injury through mitochondrial ROS. Nature 515:431-435.

de Castro Fonseca M, Aguiar CJ, da Rocha Franco JA, Gingold RN, Leite MF (2016) GPR91: expanding the frontiers of Krebs cycle intermediates. Cell Commun Signal 14:3.

Ehinger JK, Piel S, Ford R, Karlsson M, Sjövall F, Frostner E, Morota S, Taylor RW, Turnbull DM, Cornell C, Moss SJ, Metzsch C, Hansson MJ, Fliri H, Elmér E (2016) Cell-permeable succinate prodrugs bypass mitochondrial complex I deficiency. Nat Commun 7:12317.

Eltzschig HK, Eckle T (2011) Ischemia and reperfusion--from mechanism to translation. Nat Med 17:1391-1401.

Etienne-Manneville S, Hall A (2003) Cdc42 regulates GSK-3beta and adenomatous polyposis coli to control cell polarity. Nature 421:753-756.

Gibson GE, Xu H, Chen HL, Chen W, Denton TT, Zhang S (2015) Alpha-ketoglutarate dehydrogenase complex-dependent succinylation of proteins in neurons and neuronal cell lines. J Neurochem 134:86-96.

Grimolizzi F, Arranz L (2018) Multiple faces of succinate beyond metabolism in blood. Haematologica 103:1586-1592.

Harber KJ, de Goede KE, Verberk SGS, Meinster E, de Vries HE, van Weeghel M, de Winther MPJ, Van den Bossche J (2020) Succinate is an inflammation-induced immunoregulatory metabolite in macrophages. Metabolites 10:372.

Hu Z, Li F, Zhou X, Zhang F, Huang L, Gu B, Shen J, Qi S (2020) Momordica charantia polysaccharides modulate the differentiation of neural stem cells via SIRT1/B-catenin axis in cerebral ischemia/reperfusion. Stem Cell Res Ther 11:485.

Huang LY, He Q, Liang SJ, Su YX, Xiong LX, Wu QQ, Wu QY, Tao J, Wang JP, Tang YB, Lv XF, Liu J, Guan YY, Pang RP, Zhou JG (2014) ClC-3 chloride channel/antiporter defect contributes to inflammatory bowel disease in humans and mice. Gut 63:1587-1595.

Ives SJ, Zaleski KS, Slocum C, Escudero D, Sheridan C, Legesse S, Vidal K, Lagalwar S, Reynolds TH (2020) The effect of succinic acid on the metabolic profile in high-fat diet-induced obesity and insulin resistance. Physiol Rep 8:e14630.

Kamarauskaite J, Baniene R, Trumbeckas D, Strazdauskas A, Trumbeckaite S (2020) Increased succinate accumulation induces ros generation in in vivo ischemia/reperfusion-affected rat kidney mitochondria. Biomed Res Int 2020:8855585.

Kedziora KM, Leyton-Puig D, Argenzio E, Boumeester AJ, van Butselaar B, Yin T, Wu YI, van Leeuwen FN, Innocenti M, Jalink K, Moolenaar WH (2016) Rapid remodeling of invadosomes by Gi-coupled receptors: dissecting the role of Rho GTPases. J Biol Chem 291:4323-4333.

Kelly B, O'Neill LA (2015) Metabolic reprogramming in macrophages and dendritic cells in innate immunity. Cell Res 25:771-784.

Kohlhauer M, Dawkins S, Costa ASH, Lee R, Young T, Pell VR, Choudhury RP, Banning AP, Kharbanda RK, Saeb-Parsy K, Murphy MP, Frezza C, Krieg T, Channon KM (2018) Metabolomic profiling in acute ST-segment-elevation myocardial infarction identifies succinate as an early marker of human ischemia-reperfusion injury. J Am Heart Assoc 7:e007546.

Koronowski KB, Khoury N, Morris-Blanco KC, Stradecki-Cohan HM, Garrett TJ, Perez-Pinzon MA (2018) Metabolomics based identification of SIRT5 and protein kinase C epsilon regulated pathways in brain. Front Neurosci 12:32.

Li F, He X, Ye D, Lin Y, Yu H, Yao C, Huang L, Zhang J, Wang F, Xu S, Wu X, Liu L, Yang C, Shi J, He X, Liu J, Qu Y, Guo F, Zhao J, Xu W, et al. (2015) NADP(+)-IDH mutations promote hypersuccinylation that impairs mitochondria respiration and induces apoptosis resistance. Mol Cell 60:661-675.

Li J, Yang YL, Li LZ, Zhang L, Liu Q, Liu K, Li P, Liu B, Qi LW (2017) Succinate accumulation impairs cardiac pyruvate dehydrogenase activity through GRP91-dependent and independent signaling pathways: Therapeutic effects of ginsenoside Rb1. Biochim Biophys Acta Mol Basis Dis 1863:2835-2847.

Littlewood-Evans A, Sarret S, Apfel V, Loesle P, Dawson J, Zhang J, Muller A, Tigani B, Kneuer R, Patel S, Valeaux S, Gommermann N, Rubic-Schneider T, Junt T, Carballido JM (2016) GPR91 senses extracellular succinate released from inflammatory macrophages and exacerbates rheumatoid arthritis. J Exp Med 213:1655-1662.

Liu X, Zhu C, Zha H, Tang J, Rong F, Chen X, Fan S, Xu C, Du J, Zhu J, Wang J, Ouyang G, Yu G, Cai X, Chen Z, Xiao W (2020) SIRT5 impairs aggregation and activation of the signaling adaptor MAVS through catalyzing lysine desuccinylation. EMBO J 39:e103285.

Mills EL, Harmon C, Jedrychowski MP, Xiao H, Garrity R, Tran NV, Bradshaw GA, Fu A, Szpyt J, Reddy A, Prendeville H, Danial NN, Gygi SP, Lynch L, Chouchani ET (2021) UCP1 governs liver extracellular succinate and inflammatory pathogenesis. Nat Metab 3:604-617.

Nobes CD, Hall A (1995) Rho, rac, and cdc42 GTPases regulate the assembly of multimolecular focal complexes associated with actin stress fibers, lamellipodia, and filopodia. Cell 81:53-62.

Park J, Chen Y, Tishkoff DX, Peng C, Tan M, Dai L, Xie Z, Zhang Y, Zwaans BM, Skinner ME, Lombard DB, Zhao Y (2013) SIRT5-mediated lysine desuccinylation impacts diverse metabolic pathways. Mol Cell 50:919-930.

Peruzzotti-Jametti L, Bernstock JD, Vicario N, Costa ASH, Kwok CK, Leonardi T, Booty LM, Bicci I, Balzarotti B, Volpe G, Mallucci G, Manferrari G, Donegà M, Iraci N, Braga A, Hallenbeck JM, Murphy MP, Edenhofer F, Frezza C, Pluchino S (2018) Macrophage-derived extracellular succinate licenses neural stem cells to suppress chronic neuroinflammation. Cell Stem Cell 22:355-368.e13.

Prabakaran S, Vitter S, Lundberg G (2022) Cardiovascular disease in women update: ischemia, diagnostic testing, and menopause hormone therapy. Endocr Pract 28:199-203.

Reinhard NR, Mastop M, Yin T, Wu Y, Bosma EK, Gadella TWJ, Jr., Goedhart J, Hordijk PL (2017) The balance between Gα(i)-Cdc42/Rac and Gα(1)(2)/(1)(3)-RhoA pathways determines endothelial barrier regulation by sphingosine-1-phosphate. Mol Biol Cell 28:3371-3382.

Ren S, Yang M, Yue Y, Ge F, Li Y, Guo X, Zhang J, Zhang F, Nie X, Wang S (2018) Lysine succinylation contributes to aflatoxin production and pathogenicity in aspergillus flavus. Mol Cell Proteomics 17:457-471.

Rubic T, Lametschwandtner G, Jost S, Hinteregger S, Kund J, Carballido-Perrig N, Schwärzler C, Junt T, Voshol H, Meingassner JG, Mao X, Werner G, Rot A, Carballido JM (2008) Triggering the succinate receptor GPR91 on dendritic cells enhances immunity. Nat Immunol 9:1261-1269.

Sadhukhan S, Liu X, Ryu D, Nelson OD, Stupinski JA, Li Z, Chen W, Zhang S, Weiss RS, Locasale JW, Auwerx J, Lin H (2016) Metabolomics-assisted proteomics identifies succinylation and SIRT5 as important regulators of cardiac function. Proc Natl Acad Sci U S A 113:4320-4325.

Schindelin J, Arganda-Carreras I, Frise E, Kaynig V, Longair M, Pietzsch T, Preibisch S, Rueden C, Saalfeld S, Schmid B, Tinevez JY, White DJ, Hartenstein V, Eliceiri K, Tomancak P, Cardona A (2012) Fiji: an open-source platform for biological-image analysis. Nat Methods 9:676-682.

Tannahill GM, Curtis AM, Adamik J, Palsson-McDermott EM, McGettrick AF, Goel G, Frezza C, Bernard NJ, Kelly B, Foley NH, Zheng L, Gardet A, Tong Z, Jany SS, Corr SC, Haneklaus M, Caffrey BE, Pierce K, Walmsley S, Beasley FC, et al. (2013) Succinate is an inflammatory signal that induces IL-1β through HIF-1α. Nature 496:238-242.

Trauelsen M, Hiron TK, Lin D, Petersen JE, Breton B, Husted AS, Hjorth SA, Inoue A, Frimurer TM, Bouvier M, O'Callaghan CA, Schwartz TW (2021) Extracellular succinate hyperpolarizes M2 macrophages through SUCNR1/GPR91-mediated Gq signaling. Cell Rep 35:109246.

Wang T, Xu YQ, Yuan YX, Xu PW, Zhang C, Li F, Wang LN, Yin C, Zhang L, Cai XC, Zhu CJ, Xu JR, Liang BQ, Schaul S, Xie PP, Yue D, Liao ZR, Yu LL, Luo L, Zhou G, et al. (2019) Succinate induces skeletal muscle fiber remodeling via SUNCR1 signaling. EMBO Rep 20:e47892.

Willmes DM, Birkenfeld AL (2013) The role of INDY in metabolic regulation. Comput Struct Biotechnol J 6:e201303020.

Xie Z, Dai J, Dai L, Tan M, Cheng Z, Wu Y, Boeke JD, Zhao Y (2012) Lysine succinylation and lysine malonylation in histones. Mol Cell Proteomics 11:100-107.

Yang Y, Gibson GE (2019) Succinylation links metabolism to protein functions. Neurochem Res 44:2346-2359.

Yang Y, Zhang K, Chen X, Wang J, Lei X, Zhong J, Xian J, Quan Y, Lu Y, Huang Q, Chen J, Ge H, Feng H (2019) SVCT2 promotes neural stem/progenitor cells migration through activating CDC42 after ischemic stroke. Front Cell Neurosci 13:429.

Zhang Y, Zhang M, Zhu W, Yu J, Wang Q, Zhang J, Cui Y, Pan X, Gao X, Sun H (2020) Succinate accumulation induces mitochondrial reactive oxygen species generation and promotes status epilepticus in the kainic acid rat model. Redox Biol 28:101365.

Zhang Z, Tan M, Xie Z, Dai L, Chen Y, Zhao Y (2011) Identification of lysine succinylation as a new post-translational modification. Nat Chem Biol 7:58-63.

Zhu R, Zeng Q, Huang GZ, Zhong Z, Xu YG, Huang ZZ (2021) Ferroptosis and stroke. Zhongguo Zuzhi Gongcheng Yanjiu 25:3734-3739.

C-Editor: Zhao M; S-Editors: Yu J, Li CH; L-Editors: McRae M, Song LP; T-Editor: Jia Y

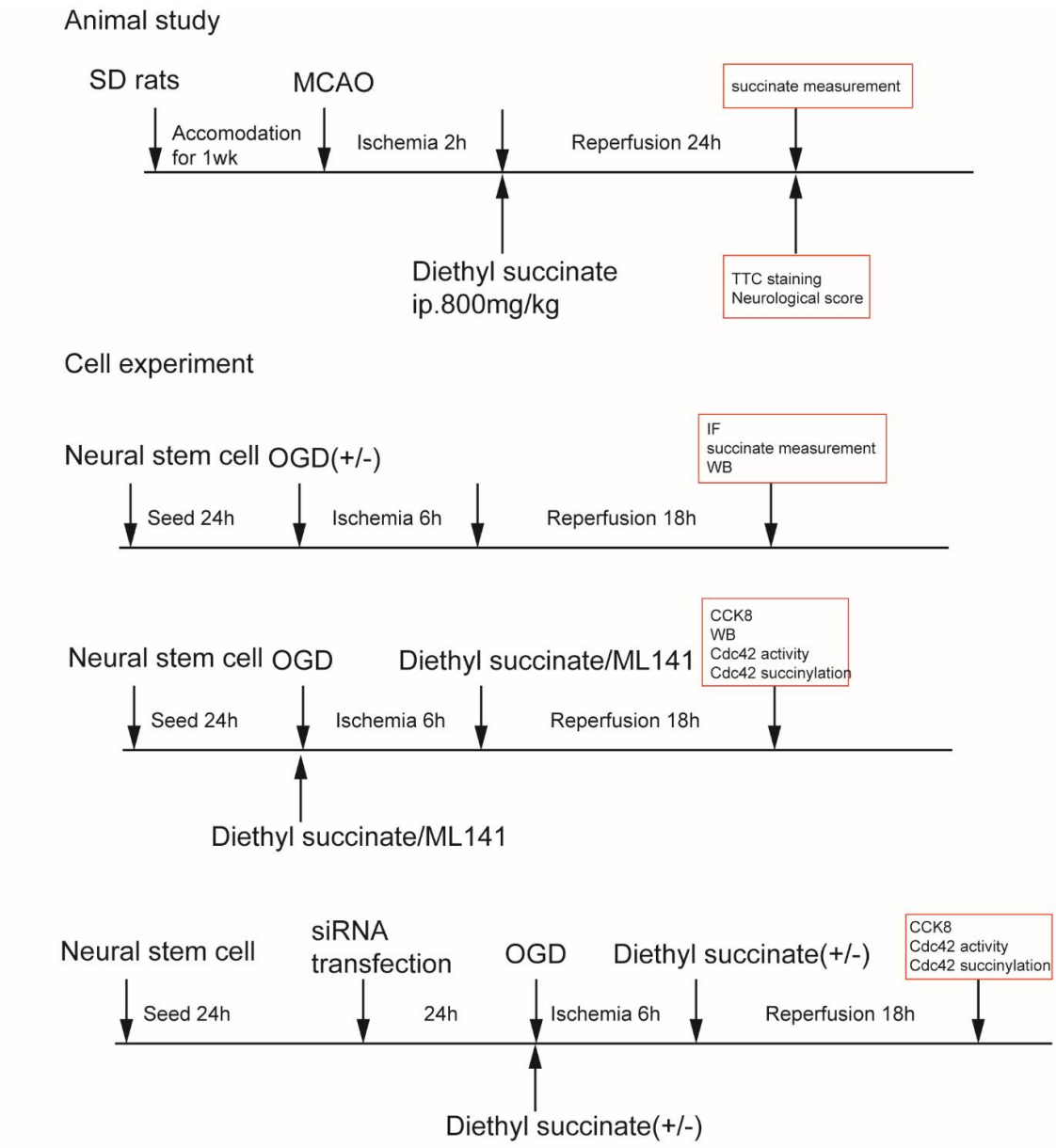

Additional Figure 1. Experimental design and timeline.

CCK8: Cell counting kit; i.p: intraperitoneal injection; IF: immunofluorescence; MCAO: middle cerebral artery occlusion; OGD: oxygen-glucose deprivation; WB: western blot.

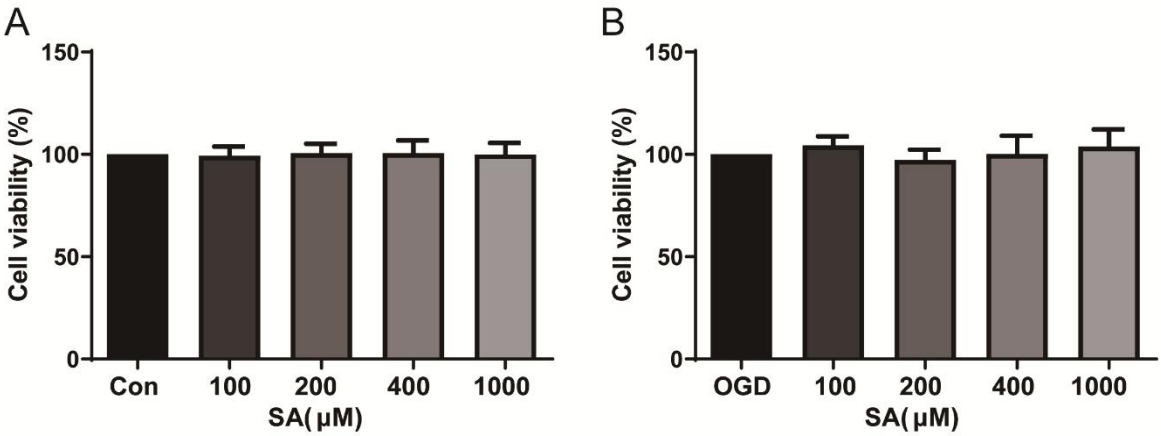

Additional Figure 2. Different concentrations of succinic acid (SA) have no effect on C17.2 cell proliferation.
(A) Physiological condition. (B) Oxygen-glucose deprivation (OGD) condition. The experiment was measured by cell counting kit 8 assay and repeated three times. Data are expressed as the mean ± SD and were analyzed by one-way analysis of variance followed by Dunnett's *post hoc* test.